Investigating the Effect of Chemotherapy on Fibroblast Activation in Triple Negative Breast Cancer Tissue

---

A thesis submitted by

Liyi Peng

in partial fulfillment of the requirements for the degree of

Master of Science

in

Biomedical Engineering

Tufts University

May 2025

Advisor: Madeleine J. Oudin, PhD

Thesis Committee:

Madeleine J. Oudin, PhD

Charlotte Kuperwasser, PhD

Shelly Peyton, PhD

ABSTRACT

Breast cancer is the most commonly diagnosed malignancy affecting women worldwide, it is the second leading cause of cancer-associated death. Triple-negative breast cancer (TNBC), accounting for 15 to 20% of cases, is an aggressive subtype of breast cancer lacking ER, PR and HER2, indicating rapid tumor progression and limited treatment options. TNBC exhibits initial sensitivity to chemotherapy but often develops chemoresistance, a process influenced by both tumor intrinsic and extrinsic factors. Here, we focused on understanding the role of the extracellular matrix (ECM), which is predominantly (~60%) produced by fibroblasts, in chemoresistance in TNBC. This study aimed to investigate chemotherapeutic effect on fibroblast and the fibroblast-derived ECM, and consequent influence on tumor cell invasion. Utilizing a sequential treatment mimicking the clinically relevant AC-T chemotherapy therapy, we found that fibroblasts were activated by chemotherapy. Further, we investigated the activation of fibroblasts *in vivo* after chemotherapy treatment. Overall, our results provide further evidence that chemotherapy can activate fibroblasts in the tumor microenvironment to produce pro-invasive changes in ECM that may contributed to poor outcomes.

ACKNOWLEDGMENTS

I would not be where I am today without the incredible support and guidance I have received throughout my degree. First and foremost, I would like to express my deepest gratitude to my advisor, Madeleine Oudin, for her unwavering support. You have been an inspiring role model both in research and in life. Thank you for guiding me through challenges, shaping my scientific journey, and always encouraging me to grow. I would also like to extend my sincere appreciation to my committee members, Shelly Peyton and Charlotte Kuperwasser, for their valuable time, insights, and support. Your guidance has been instrumental in shaping my research.

To my parents, thank you for always supporting my academic pursuits, no matter where they have taken me. Your unwavering encouragement has given me the strength to chase my dreams despite any obstacles. I am forever grateful for both your emotional and practical support. To my dear friend Siria, thank you for always being there for me, even from afar. Your constant support and friendship mean the world to me, and I deeply admire you. And Artem, I am so grateful to have had you by my side throughout the years.

To my lab mates, thank you for making the past year such a rewarding and enjoyable experience. Anna, I truly appreciate your guidance and support, as well as the invaluable research skills you have shared with me. Crystal, Hanan, and Tom, I admire your intelligence and kindness, and I look forward to witnessing your future accomplishments. Haley, Ankit, and Audrey, thank you for always being so helpful and supportive in the lab.

I am incredibly fortunate to have had such a strong network of mentors, colleagues, friends, and family throughout this journey. Thank you all for being part of it.

Table of Contents

LIST OF FIGURES

Chapter 1: Introduction

1.1 Breast Cancer and Triple-Negative Breast Cancer

Breast cancer is the most common cancer among women, surpassing lung cancer as the leading cause of global cancer incidence in 2020[1]. It accounts for approximately 1 in 4 female cancer cases and 1 in 6 female cancer deaths, ranking first in incidence across 159 of 185 countries and first in mortality in 110 countries. In the United States, breast cancer constitutes about 33% of all new female cancers each year[2], with approximately 1 in 43 women dying from the disease over their lifetime[3]. The incidence, diagnosis, and mortality rates of breast cancer vary significantly due to factors such as age, race, ethnicity and subtypes.

Breast cancer is a heterogeneous disease classified into molecular subtypes based on the immunohistochemical (IHC) expression of hormone receptors and HER2 status. These subtypes include estrogen receptor-positive (ER+), progesterone receptor-positive (PR+), human epidermal growth factor receptor 2-positive (HER2+), and triple-negative breast cancer (TNBC), which lacks expression of ER, PR, and HER2[4]. Among

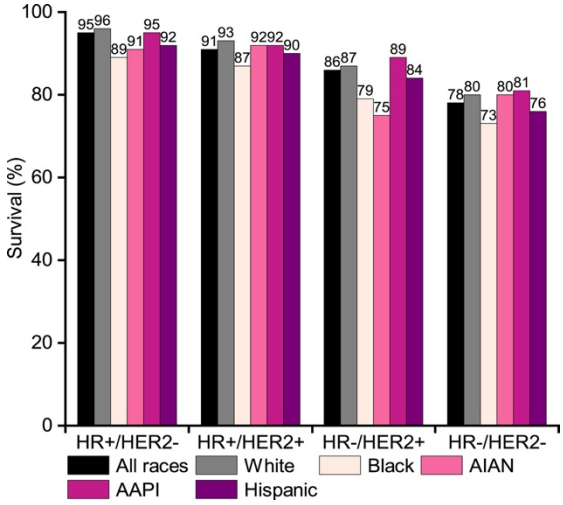

Figure 1.1 Survival of breast cancer subtypes by racial groups[5]. AAPI indicates Asian American/Pacific Islander; AIAN, American Indian/Alaska Native.

these, TNBC is associated with the poorest prognosis and lower survival rates across racial groups, with Black women having the lowest 5-year relative survival rate (73%) compared to AAPI women, who have the highest survival rate (81%) (Figure 1.1).

Triple-negative breast cancer (TNBC) is an aggressive subtype with ER-negative, PR-negative, and HER2-negative, accounting for about 10-15% of all breast cancer[6]. Compared to other subtypes, TNBC tumors are more likely to be high-grade, rapidly proliferating, and invasive, often presenting with larger tumor sizes and a higher risk of early recurrence and distant metastasis[7], which refers to the spread of cancer cells from the primary tumor to other parts of the body, forming new tumors in different organs or tissues, a process which is dependent on cell migration. Approximately 40% of patients experience recurrence within five years[22]. Common metastatic sites include visceral organs such as the liver and lungs, contributing to a 5-year survival rate of approximately 77% for localized TNBC and a median survival of only 8 to 13 months once metastasized[6,7]. Due to limited therapeutic options and poor prognosis, further research into TNBC biology and treatment is urgently needed to improve patient outcomes.

1.2 Breast cancer treatment

Breast cancer management has significantly improved, leading to an overall 5-year survival rate of approximately 91% across all[8]. Treatment strategies include local interventions such as surgery and radiation, along with systemic therapies like chemotherapy, hormone therapy, and targeted therapy[8]. However, for TNBC treatment, the options are severely limited due to its lack of hormone receptors and HER2 amplification, rendering it unresponsive to endocrine or HER2-targeted treatments.

Chemotherapy is the standard systemic treatment for TNBC, especially for metastatic TNBC[10]. Immunotherapy, a newer treatment which has shown improved survival, durable responses and fewer side effects for many cancers[40], has been investigated as an approach for TNBC treatment. The Food and Drug Administration (FDA) has approved pembrolizumab (Keytruda) targeting programmed cell death-1 (PD-1) and atezolizumab targeting programmed cell death-ligand 1 (PD-L1) for patients with advanced PD-L1-positive and early high-risk disease[41,42]. Immunotherapy in combination with other therapies modestly improves survival in metastasized and early-stage TNBC[42], while only 20-30% of TNBC cases are PD-L1-positive[43].More trials are ongoing to investigate the role of immunotherapy in TNBC. Nevertheless, chemotherapy always remains part of the treatment regimen, and the most accessible treatment option for many populations.

1.2.1 Chemotherapy for TNBC

Combined with surgery, chemotherapy, often administered post-surgery (adjuvant chemotherapy) or pre-surgery (neoadjuvant chemotherapy), plays a critical role in eliminating metastatic disease and improving survival[11]. By targeting rapidly dividing tumor cells through multiple mechanisms, including inhibiting angiogenesis, disrupting mRNA pathways, and inducing DNA damage leading to apoptosis[12].

The National Comprehensive Cancer Network (NCCN) provides a guideline for TNBC treatment to utilize therapies based on taxane, anthracycline, cyclophosphamide, cisplatin and fluorouracil[13]. Compared to single-drug treatment, multi-agent regimens have demonstrated superior efficacy, improving survival outcomes[7]. There are various combinations recommended by the NCCN, such as sequential anthracycline-

cyclophosphamide and taxane (AC-T); concurrent anthracycline-cyclophosphamide and taxane (ACT); anthracycline-cyclophosphamide without taxane (AC); cyclophosphamide, methotrexate, and fluorouracil (CMF); and docetaxel and cyclophosphamide (TC)[12,14,15]. Among these regimens, sequential anthracycline-cyclophosphamide and taxane (AC-T) is the widely accepted as standard regimen for early-stage TNBC[16-18].

The sequential anthracycline-cyclophosphamide and taxane (AC-T) therapy is a neoadjuvant chemotherapy, involving four cycles of doxorubicin and cyclophosphamide (AC phase), followed by four-time administration of paclitaxel (T phase), typically administered every three weeks[19]. AC-T therapy is effective in reducing tumor burden, improving overall survival, and minimizing toxicity through dose optimization[14,15,20]. AC-T is especially beneficial for early-stage TNBC, increasing the likelihood of achieving pathological complete response (pCR), which is correlated with better long-term outcomes.

1.2.2 Chemotherapy resistance in breast cancer

Despite its initial chemosensitivity and strong response to chemotherapy, TNBC is notorious for developing rapid resistance to chemotherapy, with chemotherapy ultimately failing to improve long-term survival, a phenomenon often referred to as the "triple-negative paradox" [21]. Approximately 40% of early-stage TNBC patients experience recurrence within the first three years post-chemotherapy[22], which significantly impacts patient quality of life and survival. Chemoresistance is a multifactorial process involving complex crosstalk between tumor cells and their microenvironment, genetic and epigenetic alterations, and activation of survival pathways[23]. Overcoming chemotherapy

resistance remains a major clinical challenge, suggesting the need to explore the underlying mechanisms that drive TNBC recurrence and resistance, with the goal of developing more effective therapeutic strategies.

1.3 Tumor microenvironment (TME)

Cancer is not just a mass of malignantly transformed cells but functions as an organ, with complex interactions between tumor cells and the surrounding tumor microenvironment (TME)[24]. While tumor cells induce physical and physiological changes within surrounding tissue to support and promote tumor growth, the tumor microenvironment, in turn, plays a significant role in promote tumor cell proliferation and invasion. Consequently, targeting tumor microenvironment has become a promising strategy for therapeutic intervention.

1.3.1 TNBC tumor microenvironment

As a dynamic network composed of various cells and other factors, tumor microenvironment is highly heterogeneous between cancer types, TNBC is characterized with unique tumor microenvironment, which differs from other subtypes of breast cancer. Because of the pivotal contribution to tumor proliferation, angiogenesis, immune evasion, and resistance to cell death, TME has been considered a feature of TNBC[25]. Rapid tumor growth in TNBC often induces hypoxia, leading to further reprogramming of the tumor and its microenvironment. This dynamic interaction creates a cycle of continuous adaptation, promoting tumor progression and metastasis[26].

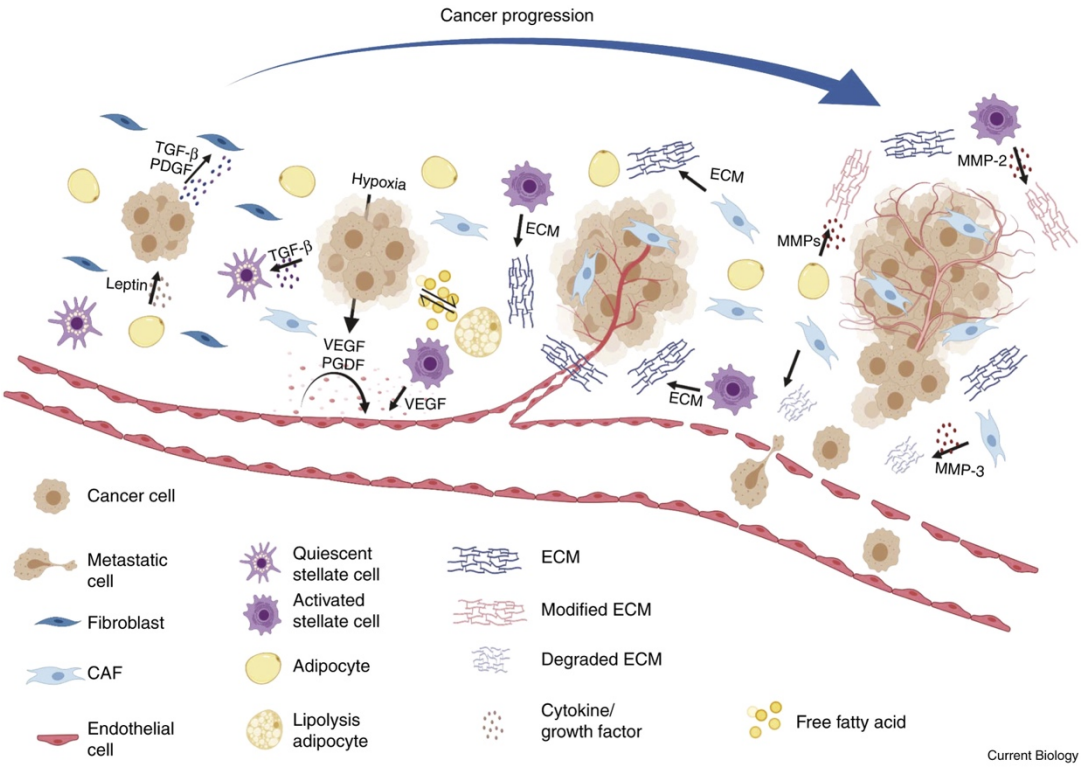

Figure 1.2 The roles of TME stromal components in tumor progression[24]

Primarily composed of immune cells, stromal cells, blood vessels, and extracellular matrix (ECM), TME affects the behaviors of tumor cells through the production of various growth factors and cytokines, facilitating tumor progression and invasion[26] (Figure 1.2). Here, we will focus on the role of the ECM.

1.3.1.1 Extracellular matrix (ECM)

Extracellular matrix (ECM), consisting of structural proteins such as collagen, fibronectin and laminin, provides physical support to tissues and regulates cellular functions. In solid tumor, up to 60% of tumor mass is constituted of ECM collagen deposits, leading to desmoplasia, which is strongly linked to poor prognosis[24]. While a few cells in the TME participate in the ECM production, cancer-associated fibroblasts (CAFs) are the primary source of ECM deposit and play a critical role in ECM remodeling.

1.3.1.2 Cancer-Associated Fibroblast

Derived from resident normal fibroblast (NFs) that undergo activation, cancer-associated fibroblasts (CAFs) are a primary component of tumor stroma, playing an important role in facilitating communication and interaction between cancer cells and TME. After being activated by various factors such as growth factors, cytokines and other molecules, fibroblasts transform into diverse subtypes of CAFs such as myofibroblastic CAFs (myCAFs) and inflammatory CAFs (iCAFs)[27]. Myofibroblasts, in particular, activated by transforming growth factor-beta (TGF-β) signaling, express high levels of alpha-smooth muscle actin (α-SMA) and serve a crucial function in proliferation, contractile properties, secretory phenotypes and extracellular matrix formation, contributing to tumor matrix remodeling[24]. Inflammatory fibroblasts, on the other hand, activated by paracrine factors from cancer cells, are characterized with low α-SMA expression and high expression of inflammatory cytokines. Both myofibroblastic and inflammatory CAFs are contributed to tumor progression. While myofibroblasts remodel ECM to promote tumor invasion and metastasis and prevent drugs as a physical barrier, inflammatory fibroblasts produce cytokines such as IL-6 to enhance drug resistance[27,39]. The abundance of CAFs within tumor has been observed to correlates with prognosis and the effect is heterogeneous depend on cancer types.

As the predominant producer of extracellular matrix in the tumor microenvironment, CAFs functionally affect tumor microenvironment through growth factors, cytokines and extracellular constituents, resulting in tumor proliferation and metastasis, neoangiogenesis, extracellular matrix remodeling and immunosuppression[24].

1.3.2 Chemotherapeutic effects on ECM composition

Emerging evidence suggests that chemotherapy not only targets tumor cells but also modifies the tumor microenvironment, potentially influencing treatment outcomes and metastasis risk. Chemotherapy has been found to involve in increasing circulating tumor cell number, suggesting it may promote distant metastasis[28]. Cytotoxic chemotherapy can induce tissue damage, hypoxia and cancer cell apoptosis, triggering the release of pro-inflammatory chemokines and cytokines from immune cells and stromal cells locally and systemically, which is called cytokine storm. This inflammatory response not only causes immunosuppression and T cell exhaustion locally, but also mobilizes bone marrow-derived progenitors to primary or secondary tumor sites, eventually creating a pro-metastatic environment[29](Figure 1.3A).

Previous study in Oudin Lab has found that cytotoxic chemotherapy can induce significant ECM changes[30]. They analyzed the composition of ECM by proteomics from PyMT-MMTV mice which develop spontaneous mammary tumors, treated with either DOX or PTX (Figure 1.3B). Principal components analysis showed significant differences between chemotherapy-treated tumor ECM and vehicle-treated ECM, while drug-specific variations were observed in doxorubicin- and paclitaxel-treated tumor tissues. Reseeding TNBC cells into decellularized scaffolds from PyMT mice tumor tissue treated with DOX or PTX led to a significant increase of tumor cell migration speed and displacement, indicating that chemotherapy-induced changes in ECM were pro-invasive (Figure 1.3C-E). They further identified Collagen IV as highly upregulated after chemotherapy treatment, which is highly associated with enhanced cancer cell invasion, potentially

leading to local invasion and metastasis. These results demonstrated that chemotherapy induces changes in ECM composition in TNBC tumors that are pro-invasive, suggesting post-chemotherapeutic TNBC tumor has a higher tendency of invasion and providing a potential mechanistic link between chemotherapy and metastasis.

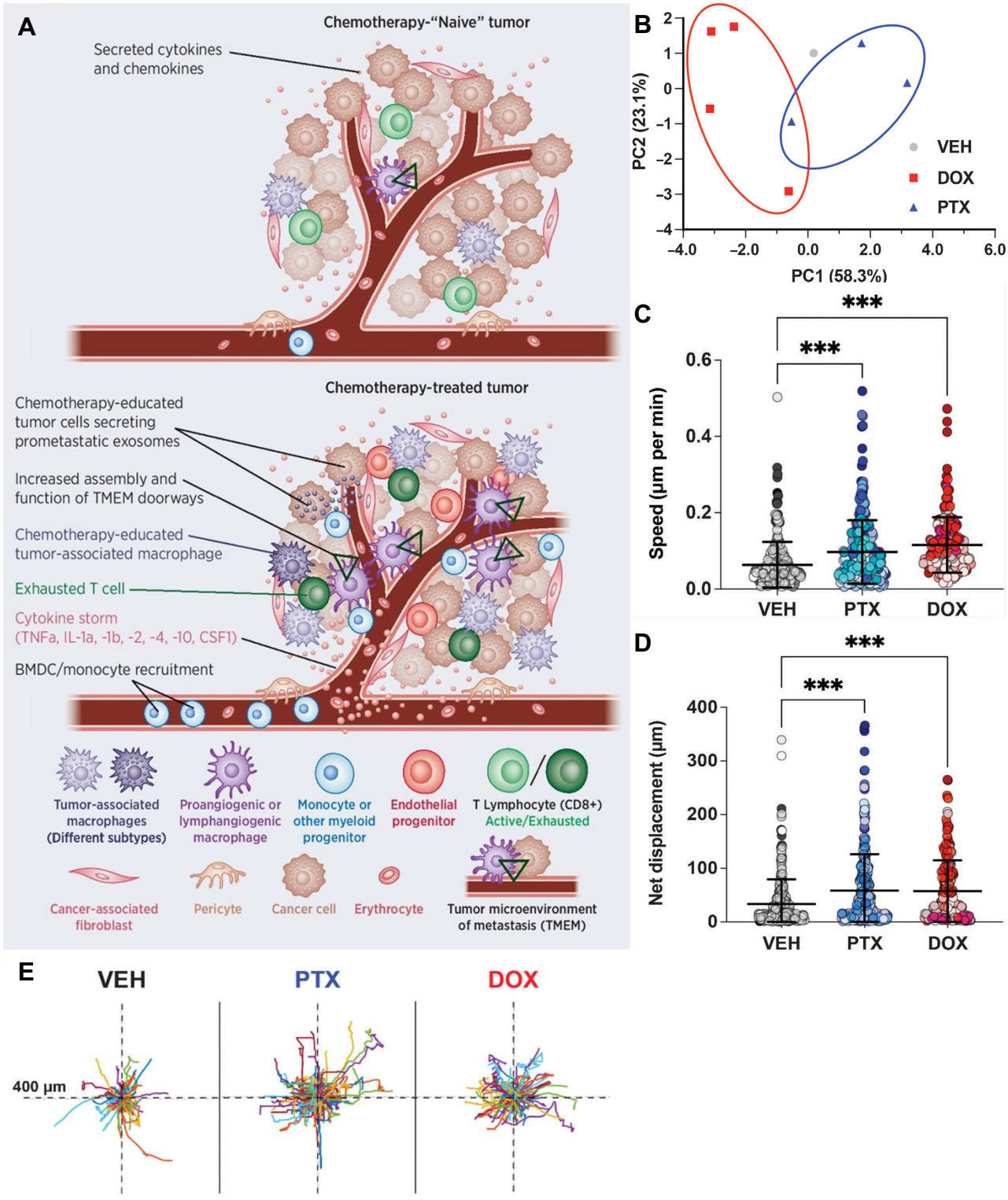

Figure 1.3 Chemotherapy induces changes in tumor microenvironment. (A) Illustration of non-treated (upper panel) and chemo-treated (lower panel) tumor microenvironment, associated with the process of metastasis[29]. (B) PCA of proteomics study investigating decellularized ECM composition from vehicle-, paclitaxel-, and doxorubicin-treated tumors. (C) Chemotherapy-treated decellularized ECM promotes motility of TNBC cells: quantification of cell motility speed and (D) displacement, (E) paths of individual cells[30].

1.4 Conclusion

While the Oudin lab has shown that chemotherapy can induce pro-invasive changes in the ECM of TNBC tumors, the mechanisms by which this occurs is not known. Identifying the mechanisms by which chemotherapy changes the ECM could lead to the development of novel therapeutic approaches, which could reduce resistance and metastatic dissemination, and improve outcomes. Given that fibroblasts are the main producers of ECM in tumors, we hypothesized that CAF activation would play an important role in chemotherapy-mediated changes in ECM. The goal of this work was to explore how chemotherapy affects fibroblast activation in TNBC tumor tissues and consequently induces ECM changes that may contribute to the development of chemoresistance. To achieve this, I performed experiments to evaluate fibroblast activation using both in vitro and in vivo models. First, I treated human fibroblasts *in vitro* with the AC-T regimen and determined the effect activation biomarker, morphology and ECM production. Then I used tissues isolated from mice treated with chemotherapy drugs including doxorubicin and paclitaxel, and evaluated fibroblast activation status in tissues.

Our observations suggest that chemotherapy enhances fibroblast activation and ECM production, which in turn promotes tumor cell motility—a key indicator of invasive potential. These results imply that chemotherapy may unintentionally remodel the tumor microenvironment in a way that facilitates tumor progression and contributes to therapeutic resistance.

Chapter 2: Evaluate the effect of combination therapy (AC-T therapy) on fibroblasts *in vitro*

2.1 Introduction

We have previously found that chemotherapy-driven compositional changes in the mammary ECM promote tumor invasion[30]. However, the mechanism by which these changes occur is still unclear. As fibroblasts are one of the primary characters contributed to the ECM, we are currently investigating the effect of chemotherapy on fibroblasts, the ECM they produce, and its effect on tumor cell properties. The Oudin lab has generated some unpublished data to investigate this. Human mammary fibroblasts isolated from healthy female breast tissue were treated with 4 different chemotherapy drugs used to treat human TNBC patients. All 4 drugs induced a significant increase in alpha-SMA, which is marker for fibroblast activation (Figure 2.1A, B). Normal fibroblasts are activated by transforming growth factor-beta (TGF-β) signaling and transform into cancer-promoting fibroblasts with high expression level of alpha-smooth muscle actin (α-SMA)[24]. In this process, Smad3, a downstream intracellular protein, is activated by phosphorylated TGF-β receptor type I (TGFBR1), resulting in the activated form phosphorylated Smad3 (pSmad3)[31]. While Smad3 is a key factor in TGF-β-mediated immunosuppression and participates in epithelial–mesenchymal transition (EMT), which is an essential step of metastasis[24,31,32], it is also responsible for regulating fibroblast activation[33,34]. In non-small cell lung cancer (NSCLC), chemotherapy drugs, including cisplatin and gefitinib, induce the increase of PD-L1 expression in cancer-associated fibroblasts, releasing elevated levels of pro-tumorigenic cytokines that promote tumor growth and chemoresistance[35]. The Oudin lab has shown that DOX and CIS increase Smad3 phosphorylation in the

activated fibroblasts (Figure 2.1C, D).

According to the guidelines provided by NCCN[13], there are various combinations of chemotherapy drugs based on taxane, anthracycline, cyclophosphamide, cisplatin and fluorouracil[12]. Generally, the mainstream combined regimens include sequential anthracycline-cyclophosphamide and taxane (AC-T); concurrent anthracycline-cyclophosphamide and taxane (ACT); anthracycline-cyclophosphamide without taxane (AC); cyclophosphamide, methotrexate, and fluorouracil (CMF); and docetaxel and cyclophosphamide (TC)[12,14,15]. Among these regimens, sequential anthracycline-cyclophosphamide and taxane (AC-T) is one of the most effective[15] and widely accepted as standard regimen for early-stage TNBC[16-18]. Therefore, we wanted to explore the effects of the clinically used AC-T therapy on fibroblast activation.

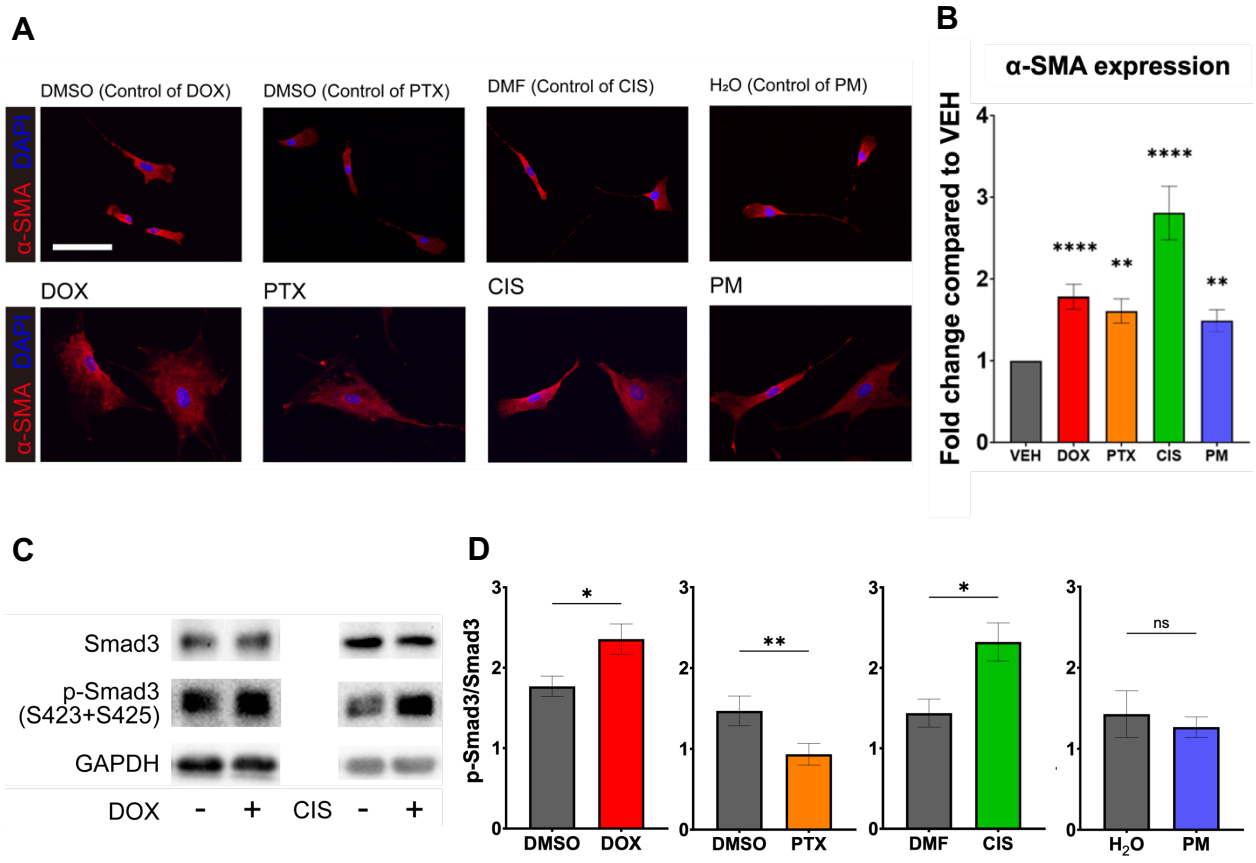

Figure 2.1 Fibroblasts are activated by chemotherapy drugs. (A) Representative images of individually chemotherapy-treated fibroblast stained for α-SMA (red) and DAPI (blue). Scale bar: 50μm. (B) Quantification of α-SMA expression level of fibroblasts. Mean ± SEM are shown. **p<0.01, ****p<0.0001 by t-test. (C) Representative Western blot images of whole cell fibroblast lysates immunoblotted for Smad3 and pSmad3. (D) Quantification of Smad3 and pSmad3 in chemotherapy-treated fibroblasts. Mean ± SEM are shown. *p<0.05, **p<0.01 by paired t-test.

2.2 Materials and Methods

2.2.1 Antibodies and drugs

Antibodies used anti-alpha smooth muscle Actin (ab7817; Abcam, Cambridge, MA), anti-Smad3 (ab40854; Abcam, Cambridge, MA), and anti-Smad3 (pS423/425), anti-fibronectin (ab194395; Abcam, Cambridge, MA), anti-GAPDH (14C10; Cell Signaling Technology). Drugs include doxorubicin (DOX) (S120814; Selleck Chemicals), phosphoramide mustard cyclohexanamine (PM) (HY-137316A; MedChemExpress) and paclitaxel (PTX) (S1150; Selleck Chemicals).

2.2.2 Cell Culture

Reduction mammary fibroblasts (RMF)[44] were a gift from Prof. Charlotte Kuperwasser's lab at Tufts University (Boston, MA), generated by primary breast fibroblasts immortalized with human telomere and GFP, and were cultured in DMEM with 10% calf serum and 1% Pen-Strep Glutamine.

MDA-MB-231 cells were obtained from ATCC (Manassas, VA), fluorescently labeled by transduction of TurboGFP-containing lentiviral particles (SHC003V; Sigma-Aldrich), were cultured in DMEM with 10% serum and Pen-Strep Glutamine.

Cells were routinely checked for the presence of mycoplasma by a PCR based method using a Universal Mycoplasma Detection Kit (30-1012K; ATCC, Manassas, VA). Only mycoplasma negative cells were used in this study.

2.2.3 Cell viability assay

Cells were seeded on 96 well polystyrene plates (4,000 cells per well) and allowed

to adhere for 24hrs. Cells were then treated with various concentrations of the combination of the three drugs (doxorubicin, phosphoramide mustard) or vehicle control, DMSO (D2650-5X10ML; Sigma-Aldrich, St. Louis, MO) for doxorubicin and paclitaxel, UltraPure™ DNase/RNase-Free Distilled Water (10977015; Thermo Fisher Scientific, Waltham, MA) for phosphoramide mustard. The schedule of treatment started from incubating with doxorubicin and phosphoramide mustard for 72 hours, followed by 72-hour incubation with media, and then incubated with paclitaxel for another 72 hours. PrestoBlue™ Cell Viability Reagent (A13261; Invitrogen, Carlsbad, CA) was added to each well according to the manufacturer's instructions and incubated for 30 min at 37°C. The absorbance of cells treated with different drug concentrations was measured on a plate reader and the viability curves were drawn according to absorbance. Based on the results, a combination of drug concentrations was determined as a standard sequential treatment for the further experiments.

2.2.4 Immunofluorescence of fibroblasts

Clear 24 well glass plates coated with 0.1% Gelatin were seeded with RMF cells (500 cells per well) and left to attach overnight. Cells were then treated with drugs (doxorubicin, phosphoramide mustard, paclitaxel) or corresponding vehicle controls, DMSO (D2650-5X10ML; Sigma-Aldrich, St. Louis, MO) for doxorubicin and paclitaxel, UltraPure™ DNase/RNase-Free Distilled Water (10977015; Thermo Fisher Scientific, Waltham, MA) for phosphoramide mustard. Cells were incubated for 9 days following the sequential treatment and then fixed using 4% PFA for 20 min. Cells were permeabilized with 0.1% triton-X, washed and the blocked with 10% normal donkey serum, and 0.2%

tween-20 at room temperature for 1 hour. Primary antibody was then added in a 1% normal donkey serum and incubated at room temperature for 1 hour. Secondaries including DAPI (nuclei) combined with Alexa Fluor 647 or Phalloidin (F-actin) were then added in a 1% normal donkey serum. Cells were then washed and imaged using the Zeiss LSM 900 confocal microscope with tile imaging, the images were processed by Zen with stitching.

2.2.5 Western Blotting

Cells were seeded into 6 well polystyrene plates (10,000 cells per well) and allowed to adhere for 24hrs. Then cells were treated with drugs (doxorubicin, phosphoramide mustard, paclitaxel) or vehicle control, DMSO (D2650-5X10ML; Sigma-Aldrich, St. Louis, MO) for doxorubicin and paclitaxel, UltraPure™ DNase/RNase-Free Distilled Water (10977015; Thermo Fisher Scientific, Waltham, MA) for phosphoramide mustard, following the sequential treatment for 9 days. Cell pellets were lysed in 25 mmol/L tris, 150 mmol/L NaCl, 10% glycerol, 1% NP-40, and 0.5 mol/L EDTA with 1× protease Mini-complete protease inhibitor (04693124001; Roche) at 4°C. The resulting lysates were then centrifuged at 14,800 rpm for 10 minutes at 4°C and the supernatant was stored at −20°C.

Protein lysates were separated using SDS- polyacrylamide gel electrophoresis on a 12% polyacrylamide gel. Proteins were transferred to a nitrocellulose membrane using a TransBlot Turbo Transfer system (Bio-Rad; Hercules, CA). Membranes were blocked in 5% bovine serum albumin in tris-buffered saline with 0.05% tween 20 and incubated in primary antibody overnight at 4 ºC with rocking. Antibody binding was visualized using

horseradish peroxidase-conjugated secondary antibodies (Jackson ImmunoResearch, West Grove, PA). Imaging was performed using a ChemiDoc MP imaging system (12,003,154; Bio-Rad, Hercules, CA).

2.2.6 Production of 3D fibroblast-derived ECM and decellularization

Fibroblast-derived ECMs were produced as described previously[37]. Briefly, fibroblasts were seeded into gelatin-glutaraldehyde cross-linking plate (200,000 cells per well) and allowed to adhere and get confluency for 24hrs. Cells were then treated with drugs (doxorubicin, phosphoramide mustard, paclitaxel) or corresponding vehicle controls, along with fresh 75 μg/mL L-Ascorbic acid (LAA) solution, following the sequential treatment for 9 days. Then cells were incubated for an extra day and proceeded to decellularization.

Cell-ECM complex was treated by 0.5% Triton X-100 in DPBS with 20mM fresh NH_4OH to remove fibroblasts and DNA-debris inside ECM was then removed after 2-day stabilization. The matrices were stored at 4 °C for future experiments.

2.2.7 Immunofluorescence of decellularized ECM

Decellularized ECMs were blocked with 10% normal donkey serum, and 0.2% tween-20 at room temperature for 1 hour. Primary antibody was then added in a 1% normal donkey serum and incubated at room temperature for 1 hour. Secondaries including DAPI (nuclei) combined with Alexa Fluor 647 were then added in a 1% normal donkey serum. ECMs were then washed and imaged using the Zeiss LSM 900 confocal microscope.

2.2.8 Decellularized ECM scaffold reseeding

Decellularized ECMs were reseeded with 5,000 231-GFP cells each well and incubated at 37 °C for 6 hours. Reseeded scaffolds were then imaged with 10X objective for 16 hours, capturing images every 20 minutes using a Keyence BZ-X710 microscope (Keyence, Elmwood Park, NJ). Cells were then tracked using VW-9000 Video Editing/Analysis Software (Keyence) based on movement of the main cell body, and speed and persistence were calculated using a custom MATLAB script vR2024b (MathWorks). Data presented are the result of at least three independent experiments with fifty fields of view imaged per experiment and up to 12 cells tracked per field of view.

2.2.9 Statistical analysis

Statistical analysis and visualization were performed using Graph-Pad Prism v9.3.1. To compare two groups, an unpaired t test was used. A P value ≤ 0.05 was considered statistically significant.

2.3 Results

2.3.1 Design of AC-T treatment schedule for fibroblast *in vitro*

Most studies that use the AC-T therapy regimen use it *in vivo*. For that reason, it is necessary to design a treatment schedule with appropriate concentrations of drugs for fibroblasts *in vitro*. Cell viability assay was used to determine concentrations of chemotherapy drugs for fibroblast treatment. Cells were treated with drugs in the AC-T therapy regimen: doxorubicin, paclitaxel (PTX) and phosphoramide mustard (PM) (active metabolite of cyclophosphamide) for 72h each (Figure 2.1A). We tried combinations of DOX, PM and PTX at different concentrations according to IC_{50} of human TNBC MDA-MB-231 cells, aiming to find a balance between drug efficacy and cell health. With increasing concentrations of DOX, PM, and PTX, cell survival demonstrated a dose-

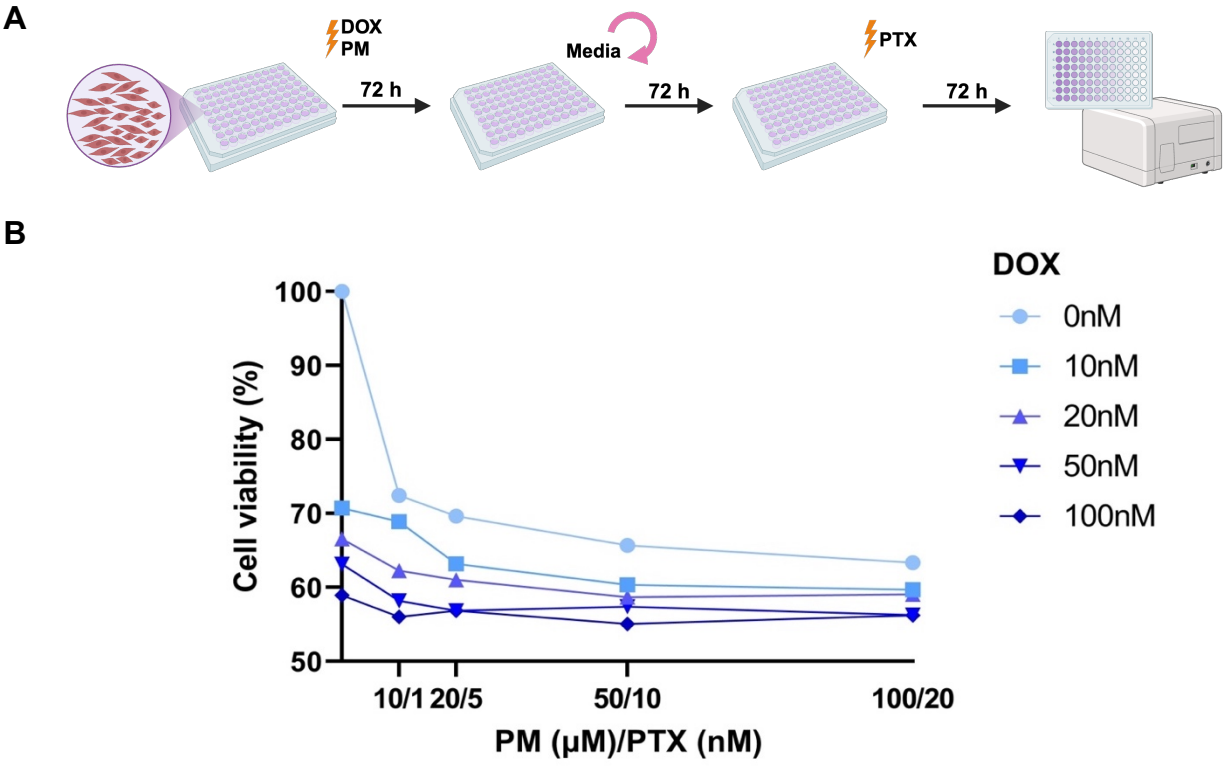

Figure 2.2 Viability assay of fibroblasts treated with AC-T therapy. (A) Schematic depiction of presto blue proliferation assay. (B) Viability curves of fibroblasts treated with chemotherapy drugs in different concentrations.

dependent decline. Within the range of concentrations tested in this experiment, fibroblast viability was maintained between 50-70%. Based on the viability results (Figure 2.1B), concentrations for each drug were selected that ensured a balance between drug efficacy and sufficient cell survival. We selected concentrations where around 60% of cells were viable after treatment. The concentration of paclitaxel was chosen to maintain consistency with previous studies. The selected concentrations were 50 nM for doxorubicin, 50 μM for phosphoramide mustard, and 5 nM for paclitaxel.

2.3.2 Increased fibroblast activation due to AC-T therapy

Based on the schedule determined in 2.3.1, fibroblasts were sequentially treated with chemotherapy drugs. To evaluate the activation of fibroblasts, I quantified α-SMA expression and Smad3 phosphorylation, and also characterized morphological changes. For morphological assessment, eccentricity was used, which is the ratio of the distance between the foci of the ellipse and its major axis length, where a perfect circle has a value of 0, and more elongated cells have a value of 1. AC-T treatment significantly increased α-SMA expression and fibroblast elongation of fibroblasts (Figure 2.2A-D). However, the phosphorylation of Smad3 was not significantly affected by AC-T treatment, doxorubicin or phosphoramide mustard, while there was significant decrease of phosphorylated Smad3 in fibroblasts treated with paclitaxel (Figure 2.2 E, F). I found that the AC-T therapy induces fibroblast activation, but that it may not be occurring through the Smad3 pathway.

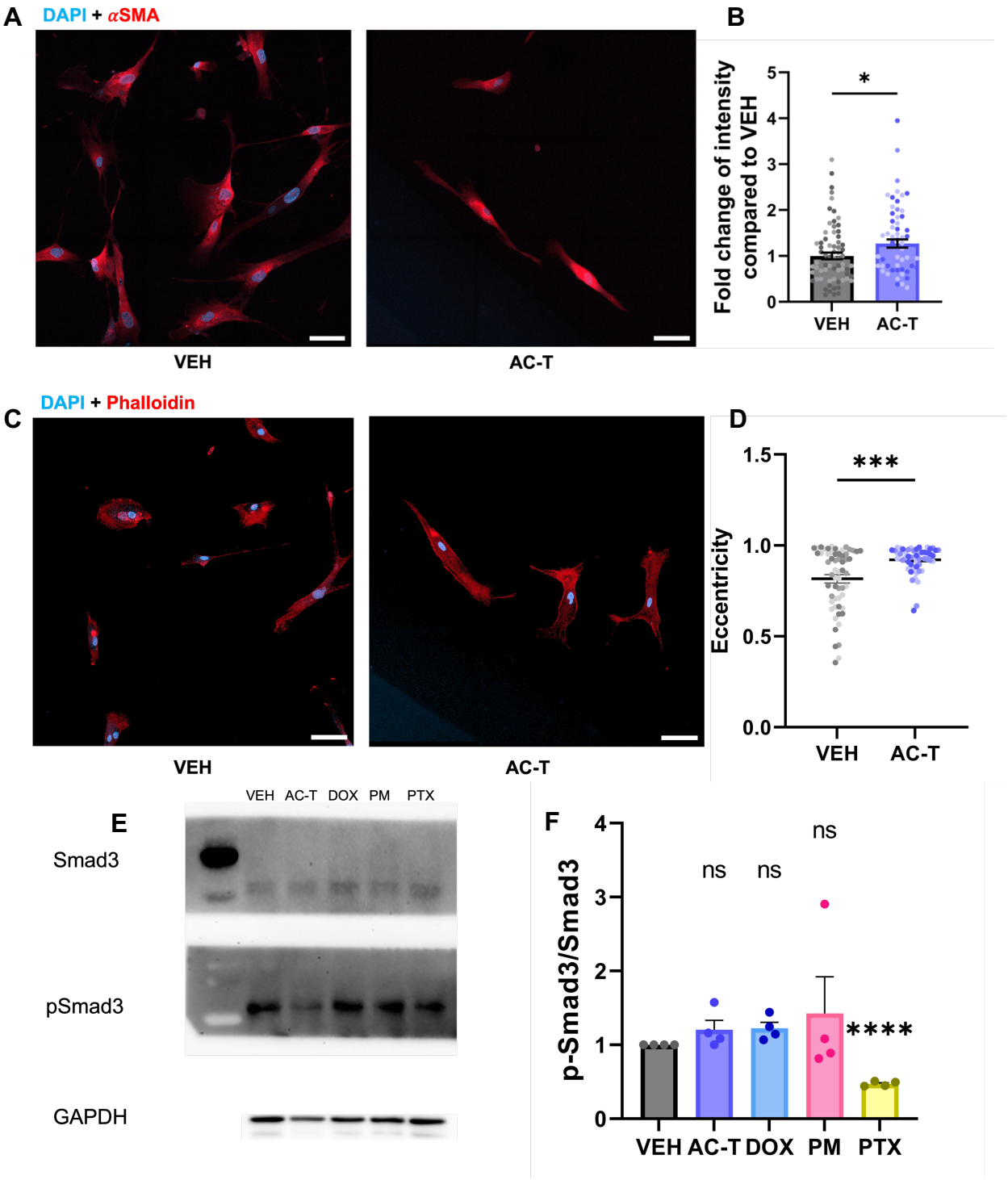

Figure 2.3 Effect of AC-T treatment on fibroblast activation *in vitro*. Representative images of fibroblasts stained for α-SMA (A)/ Phalloidin (C) (red) and DAPI (blue). Scale bar: 50μm. (B) Quantification of expression level of α-SMA. (D) Quantification of eccentricity. Significance was determined by unpaired t-test to compare between groups. (E) Representative Western blot images of whole cell fibroblast lysates immunoblotted for Smad3 and pSmad3. (F) Quantification of Smad3 and pSmad3 in chemotherapy-treated fibroblasts. A paired t-test was used to compare groups treated with different drugs. Data are shown as mean with SEM. Each data point represents a single cell, and data represents results from three independent experiments with three technical replicates.

2.3.3 ECM-driven cell invasion is increased in fibroblast-derived matrix treated with AC-T therapy

We then sought to characterize the effect of ECM generated by AC-T-treated fibroblasts on tumor cell invasion. Fibroblasts were used to generate ECM and treated with AC-T therapy during the process of ECM generation (Figure 2.3A). The fibroblast-ECM complex was decellularized and reseeded with human TNBC MDA-MB-231 cells labeled with GFP. Cell migration is important for all phases of tumor progression and can

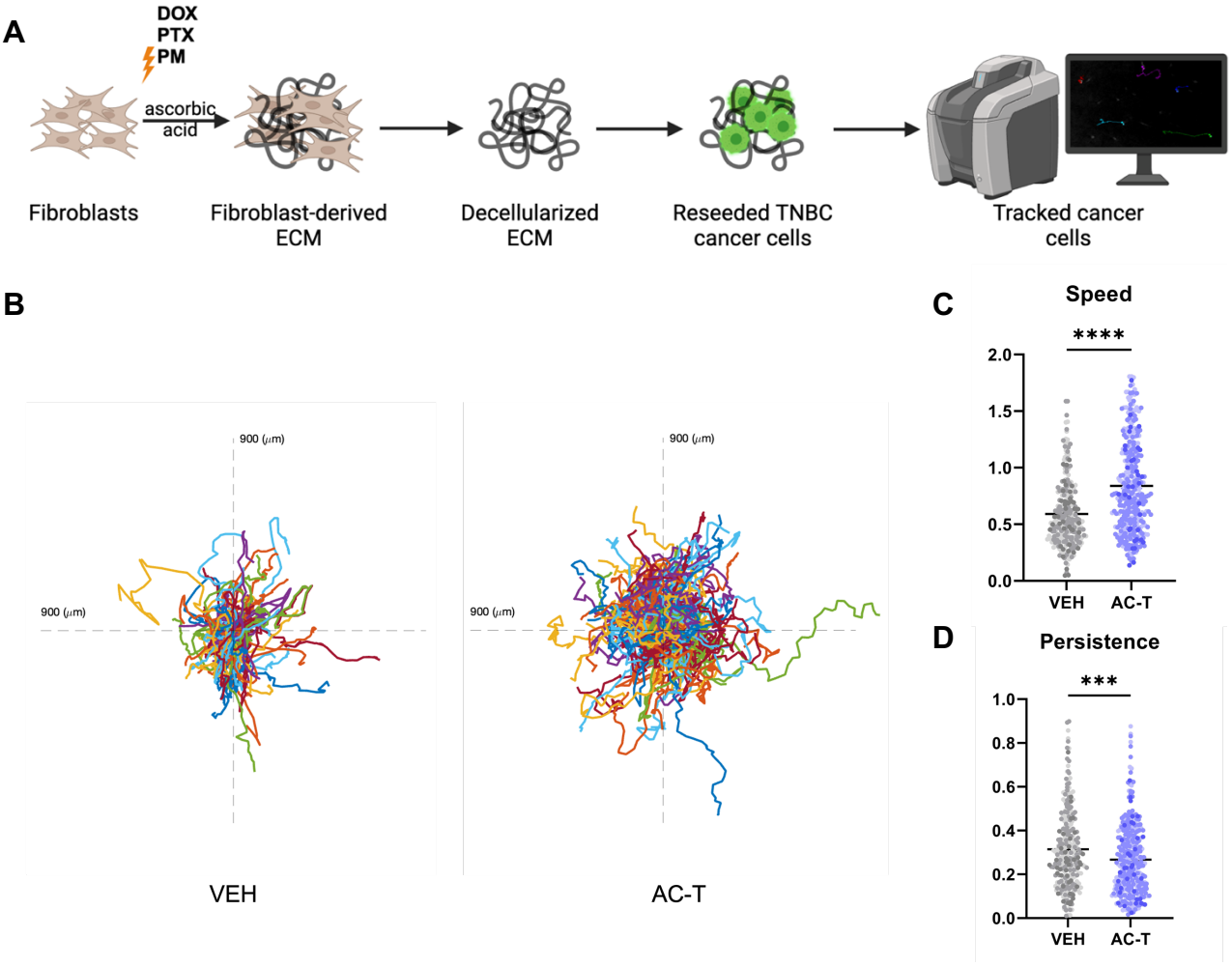

Figure 2.4 Effect of AC-T-treated fibroblast-derived ECM on TNBC cancer cell invasion. (A) Schematic depiction of ECM generation by fibroblasts. (B) Representative rose plots of MDA-MB-231 cells reseeded into fibroblast-derived ECM. (C) Cell invasion speed and (D) persistence. Significance was determined by unpaired t-test between groups (P***<0.001, P****<0.0001). Each data point represents a single cell, and data represents results from three independent experiments with three technical replicates.

be used to predict metastatic potential. A significant increase in speed was seen in the ECM obtained from AC-T-treated fibroblasts, while significant decrease was seen in persistence (Figure 2.3B-D). Overall, these results show that cancer-promoting fibroblast activated by AC-T therapy facilitate TNBC cell invasion through remodeling ECM.

2.4 Discussion

Chemoresistance is a significant issue for TNBC treatment due to the high rate of recurrence and metastasis. In this study, I aimed to investigate the effects of AC-T therapy on fibroblast activation, which is the chemotherapy regime used in the clinic for TNBC, and ECM production, to determine its impact on tumor cell invasion. First, a significant increase of α-SMA expression and elongation was seen, indicating that fibroblasts were activated by AC-T treatment. To evaluate the impacts of chemotherapy-induced fibroblast activation on tumor invasion, I produced ECM from chemotherapy-treated fibroblasts, and then reseeded TNBC cells into decellularized ECM, tracked the motility of TNBC cells within the scaffolds. In the chemotherapy-treated ECM, TNBC cells exhibited a higher intendency of invasion by the increased moving speed and range, suggesting pro-invasive effect of chemotherapy through activated fibroblasts. These results confirm that different single and combination chemotherapy regimens lead to fibroblast activation.

Previous data in the lab had shown that Paclitaxel can activate TGF-β-driven Smad3 signaling in fibroblasts, which has been shown to lead to increased ECM production. Therefore, I investigated the phosphorylation ratio of Smad3 in fibroblasts treated with the AC-T regimen and the single drug combinations and found that even though AC-T induces fibroblast activation and pro-invasive ECM changes, it does not lead to Smad3 phosphorylation. The chemotherapy-induced phosphorylation differed between this experiment and the previous study. There were some significant differences between the experimental setups of both experiments—in the previous studies, fibroblasts were treated with chemotherapy drugs for 72 hours, while here, because of the multiple different drug regimens, fibroblasts were treated for a longer duration—9 days. Further,

the chemotherapy drugs were administered sequentially. Therefore, it is possible that the single-drug treatments with doxorubicin and phosphoramide mustard, pathway activation may have decreased over time after drugs removal. While the signaling of fibroblast activation is complex, there is no effect of AC-T therapy, doxorubicin or phosphoramide mustard on Smad3 phosphorylation. TGF-β/Smad3 signaling is one of the pathways known to be involved in fibroblast activation. However, there are other pathways including Platelet-Derived Growth Factor (PDGF), Wnt signaling and Hedgehog-GLI signaling can also engage in chemotherapy-induced fibroblast activation[34,45-49]. Hedgehog (Hh) signaling is a potential pathway due to the association with EMT-transcription factors in TNBC, which can be further explored to reveal underlying mechanisms[34,53]. Given that fibroblasts promoted ECM-driven invasion following chemotherapy, despite Smad3 signaling was not activated, it suggests that fibroblasts were activated through alternative pathways.

In conclusion, based on these results, we have found that the AC-T chemotherapy regimen promotes fibroblast activation, leading to pro-invasive effects of ECM on tumor cells. To explore deeper into the impacts on TNBC tumor invasion, it is necessary to identify pathways involved in chemotherapy-driven fibroblast activation, and to focus on *in vivo* experiments using TNBC mouse models treated with AC-T therapy. For instance, investigating fibroblast activation in AC-T-treated tissues, as well as evaluating TNBC cell motility in ECM decellularized from mouse tumor, would provide beneficial insights.

2.5 Contributions to this chapter

Conception and design: Madeleine J. Oudin, Anna Yui, Liyi Peng

Acquisition of data: Liyi Peng

Analysis and interpretation of data (e.g., statistical analysis, biostatistics, computational analysis): Liyi Peng, Anna Yui

Software: Thomas Gerton

Writing, review, and/or revision of the manuscript: Liyi Peng, Anna Yui, Madeleine J. Oudin

Chapter 3: Investigate the effect of DOX and PTX on fibroblast activation *in vivo*

3.1 Introduction and Preliminary Data

We have previously found that chemotherapy-driven compositional changes in the mammary ECM promote tumor invasion[30]. However, the mechanism by which this occurs remains poorly understood. As fibroblasts are one of the primary contributors to the ECM, we are trying to find out chemotherapeutic effect on fibroblast and the ECM produced by chemotherapy-treated fibroblasts, as well as their roles in tumor progression. As shown in chapter 2, the unpublished data in the Oudin lab has found that several chemotherapy drugs used in TNBC treatment facilitate fibroblast activation and affect relevant signaling pathway activation (Figure 2.1). Whether chemotherapy drugs induce fibroblast activation *in vivo* has not been examined. The goal of this part of the project is to investigate whether chemotherapy treatment in vivo induces fibroblast activation.

Chemotherapy is a systemic treatment, which affects not only the tumor but also distant healthy tissues. Activated fibroblasts in healthy tissue potentially alter the environment to promote tumor invasion[54]. To investigate effects of chemotherapy on fibroblast activation in both TNBC tumor and healthy breast tissue, I used tissue slides obtained from multiple mouse models, including healthy fat pads from FVB/NJ mice, tumors from C57BL/6 mice orthotopically injected EO771 cells and transgenic MMTV-PyMT mice which spontaneously develop tumors commonly used as TNBC mouse model. These mice had been treated with doxorubicin, paclitaxel or corresponding controls respectively. The expression levels of primary ECM components (Collagen IV and VI) and proteins related to fibroblast activation (α-SMA, Smad3 and phosphorylated Smad3) were

evaluated by quantifying the immunostaining images. Collagen IV is one of the major components of basement membranes, while collagen VI forms a microfibrillar network and facilitates connections between cells and matrix components[50,51]. Both collagen IV and VI are known to be affected by chemotherapy and drive tumor cell invasion [30,52]. By assessing the ECM compositional changes in healthy and tumor-bearing mice treated with chemotherapy drugs, the chemotherapeutic effects found in the previous study[30] can be further verified. Additionally, through examining biomarker of activated fibroblasts and Smad3 phosphorylation conducted by fibroblasts, I aimed to characterize the chemotherapeutic effects on fibroblast activation *in vivo*.

3.2 Materials and Methods

3.2.1 Antibodies

Antibodies used anti-alpha smooth muscle Actin (ab7817; Abcam, Cambridge, MA), anti-collagen IV (ab6586; Abcam, Cambridge, MA), anti-collagen VI (ab199720; Abcam, Cambridge, MA), anti-Smad3 (ab40854; Abcam, Cambridge, MA), and anti-Smad3 (pS423/425).

3.2.2 Histological studies

Tissue blocks from the previous study in the Oudin lab[30] were used. Female transgenic mice bearing the polyomavirus middle T antigen under control of the mouse mammary tumor virus promoter (MMTV-PyMT), female C57Bl/6 and FVB/NJ mice were obtained from The Jackson Laboratory. MMTV-PyMT mice were grown until overall tumor burden reached 500 mm^3 at about 10 to 12 weeks of age before being randomized into chemotherapy treatment groups. Doxorubicin (Adriamycin) was dissolved in PBS and administered intravenously at 5 mg/kg. Paclitaxel (Taxol) was resuspended in 5% dimethyl sulfoxide, 40% polyethylene glycol 3000, and 5% Tween 80 in dH_2O and administered intraperitoneally at 10 mg/kg. Appropriate vehicle controls for each drug were included in the control group. All drugs were administered for four cycles given every 5 days. Tumor burden was monitored using digital calipers at each treatment. Three days after the final treatment, mice were euthanized, and tumors were excised for further study.

Tissue blocks from Prof. Alcaide's lab at the School of Medicine in Tufts University were also included in this study. C57BL/6 mice were injected into 4^{th} left fat pad with

EO771 cells at about 5 weeks of age before being randomized into chemotherapy treatment groups. Doxorubicin was dissolved in PBS and administered intraperitoneally at 5 mg/kg for five cycles given every 5 days, while PBS were used with 200 μg of IgG (BioXCell, BE0089) in the control group. Mice were euthanized at about 9 weeks of age and tumors were excised for further study.

Tissue blocks from previous unpublished study in the Oudin lab were used as well. FVB/NJ mice were obtained from Jackson Laboratories (Bar Harbor, ME) at 12 weeks old. Doxorubicin was dissolved in PBS and administered intravenously at 1.25mg/mL. Paclitaxel was resuspended in 1% dimethyl sulfoxide, 3% polyethylene glycol 400, and 5% Tween 80 in PBS and administered intraperitoneally at 2.5 mg/mL. Appropriate vehicle controls for each drug were included in the control group. All drugs were administered for four cycles given every 5 days.

3.2.3 Immunofluorescence of tissue sections

Tumors dissected from MMTV-PyMT and C57BL/6 mice and mammary fat pads dissected from FVB mice were fixed in 4% paraformaldehyde in PBS and embedded in paraffin. For immunofluorescence, tissue sections were deparaffinized followed by antigen retrieval using Citra Plus solution (HK057; Biogenex, Fremont, CA). After blocking in PBS-0.5% Tween 20 and 10% normal donkey serum, sections were incubated with primary antibodies overnight at 4°C and fluorescently labeled secondary antibodies at room temperature for 2 hours. 4',6-diamidino-2-phenylindole (DAPI; D1306; Thermo Fisher Scientific, Waltham, MA) was used to stain cell nuclei, and fluorochromes on secondary antibodies included Alexa Fluor 647 (Jackson ImmunoResearch, West Grove,

PA). Sections were mounted in Fluoromount mounting medium (00-4958-02; Thermo Fisher Scientific, Waltham, MA) and imaged using the Zeiss LSM 900 confocal microscope with a 20X objective, capturing ten fields of view per section. Quantification of α-SMA, Collagen IV, Collagen VI signal was performed by measuring positive area, while the quantification of Smad3 and pSmad3 signal was performed by measuring area of α-SMA positivity using ImageJ (National Institutes of Health, Bethesda, MD).

3.2.4 Statistical analysis

Statistical analysis and visualization were performed using Graph-Pad Prism v9.3.1. To compare two groups, an unpaired t test was used. A P value ≤ 0.05 was considered statistically significant.

3.3 Results

3.3.1 Effect of chemotherapy on ECM protein abundance

In the previous study, the increase of ECM component (collagen IV) post chemotherapy has been reported in the PyMT-MMTV mouse model treated with DOX and PTX [30]. I evaluated the abundance of primary ECM components, Collagen IV and VI, in the mammary gland of healthy mice and in mammary tumors generated by injection of EO771 cells into C57Bl6 mice. Due to the availability of tissue blocks treated only with

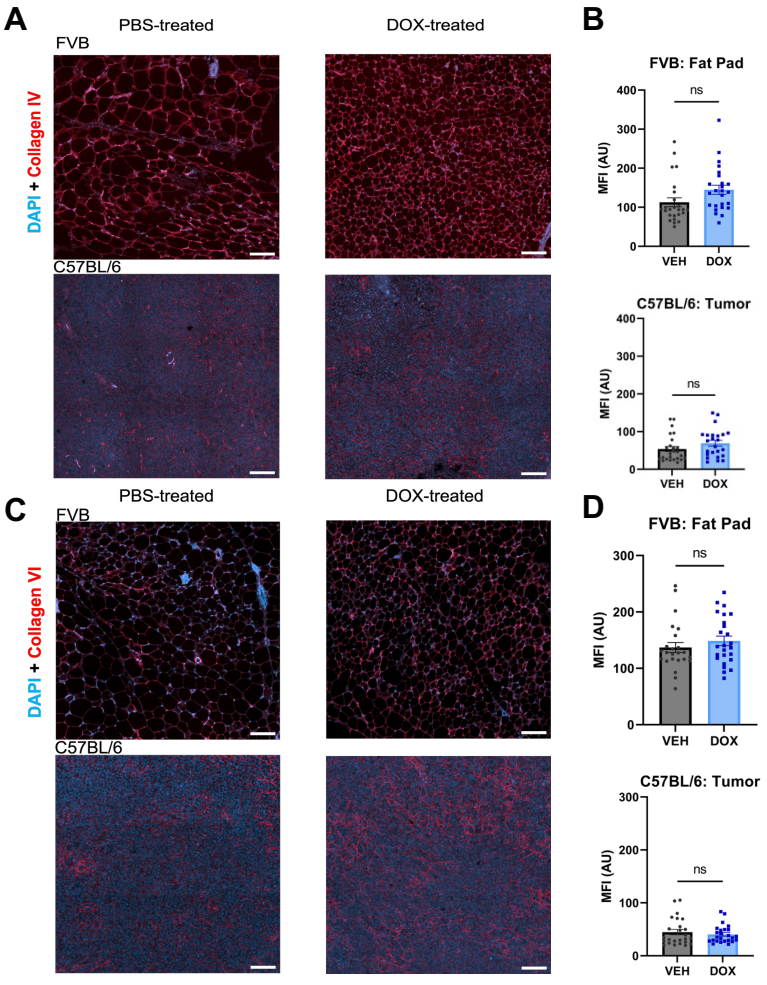

Figure 3.1 Effect of Doxorubicin on abundance of Collagen IV and VI. Representative images of FVB fat pads and C57 tumors stained for (A) Collagen IV/ (C) VI (red) and DAPI (blue). Scale bar: 50µm. Quantification of expression level of Collagen IV (B) and IV (D). Data are shown as mean with SEM, each data point represents the mean of one field of view per animal with SD n=3 animals/ group.

DOX from collaborators, this experiment focused exclusively on DOX-treated tumors. No significant difference between DOX-treated tissues and controls was observed in the abundance of collagen IV and VI (Figure 3.2).

3.3.2 Chemotherapeutic effect on fibroblast activation

To investigate whether chemotherapy treatment induces fibroblast activation in vivo, we assessed the area of α-SMA within a tumor section, one of the biomarkers of fibroblast activation in healthy fat pads and tumors from spontaneous (MMTV-PyMT) and orthotopic (C57BL/6) tumor-bearing mice, treated with doxorubicin, paclitaxel or their controls. The α-SMA-positive area was significantly increased in doxorubicin-treated tumors from C57BL/6 mice. In contrast, no significant differences were observed in healthy fat pads or spontaneous tumors following treatment with either doxorubicin or paclitaxel. These finding suggest that doxorubicin promotes fibroblast activation specifically in orthotopically formed tumor (Figure 3.3A, B).

Additionally, a locational difference in α-SMA expression was observed particularly in tumors from MMTV-PyMT mice, in both chemotherapy-treated and control groups (Figure 3.3C). Compared to the central area of tumor with low α-SMA expression, the periphery of tumor was seen to express higher α-SMA, implying that there is potentially peripheralization of fibroblasts within tumor.

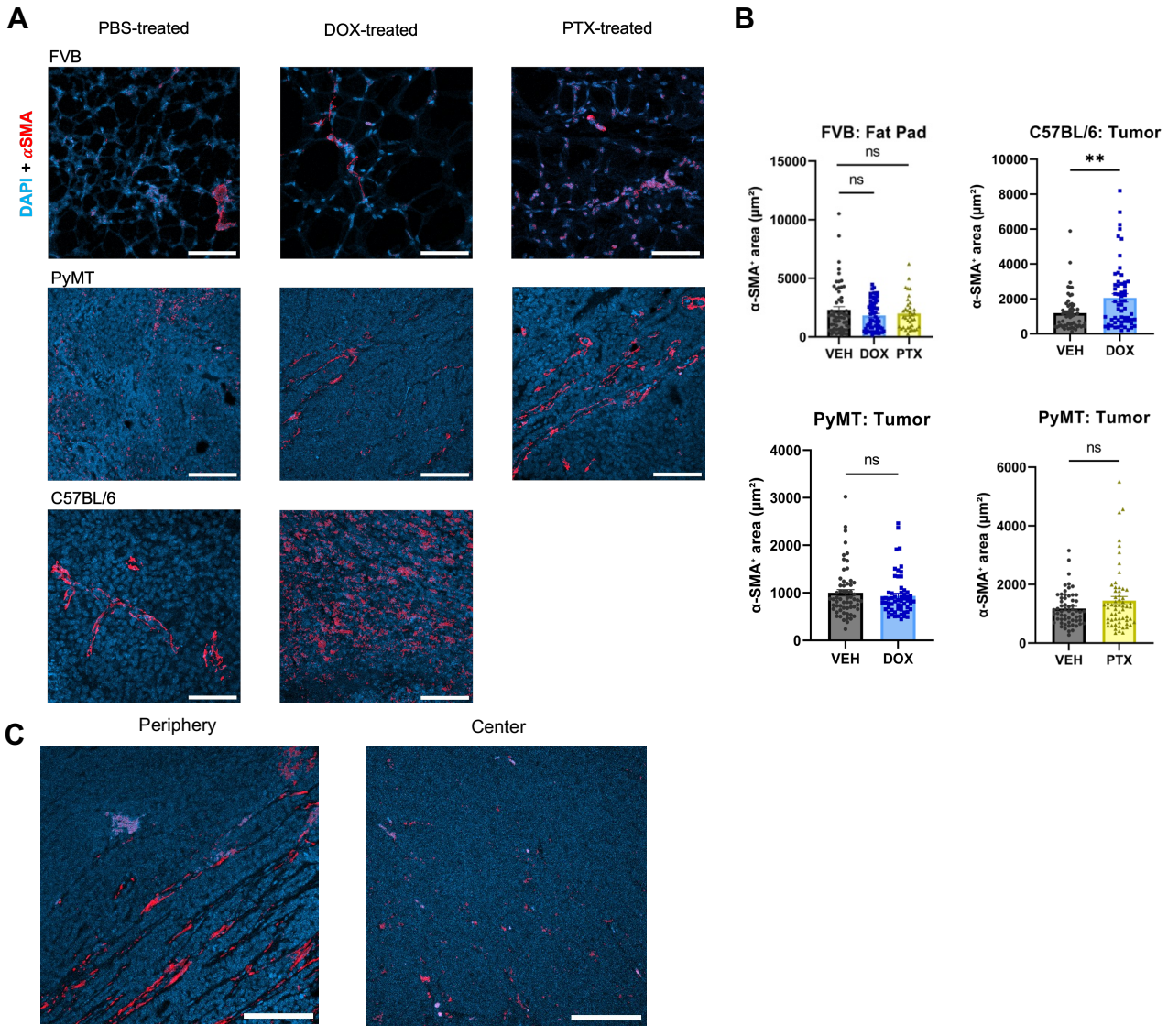

Figure 3.2 Effect of chemotherapy on expression of α-SMA. (A) Representative images of FVB fat pads, C57 and PyMT tumors stained for α-SMA (red) and DAPI (blue). Scale bar: 100μm. (B) Quantification of α-SMA. (C) Representative images of α-SMA locational difference in PyMT tumor. Data are shown as mean with SEM, each data point represents the mean of one field of view per animal. n=3 animals per group.

We also investigated the expression level of Smad3 and phosphorylated Smad3 in healthy fat pads and tumors (Figure 3.4A, Figure 3.5A). To characterize fibroblast-induced Smad3 phosphorylation, I evaluated Smad3 and pSmad3 expression within α-SMA-positive area in the images. Doxorubicin and paclitaxel treatments increased Smad3 expression in healthy fat pads. Paclitaxel treatment also decreased pSmad3 expression in fat pads, whereas doxorubicin treatment did not affect pSmad3 levels. In orthotopic and spontaneous tumors, doxorubicin treatment did not affect Smad3 or pSmad3 expression. Additionally, paclitaxel decreased both Smad3 and pSmad3 expression in spontaneous tumor significantly (Figure 3.4B, C, Figure 3.5B, C).

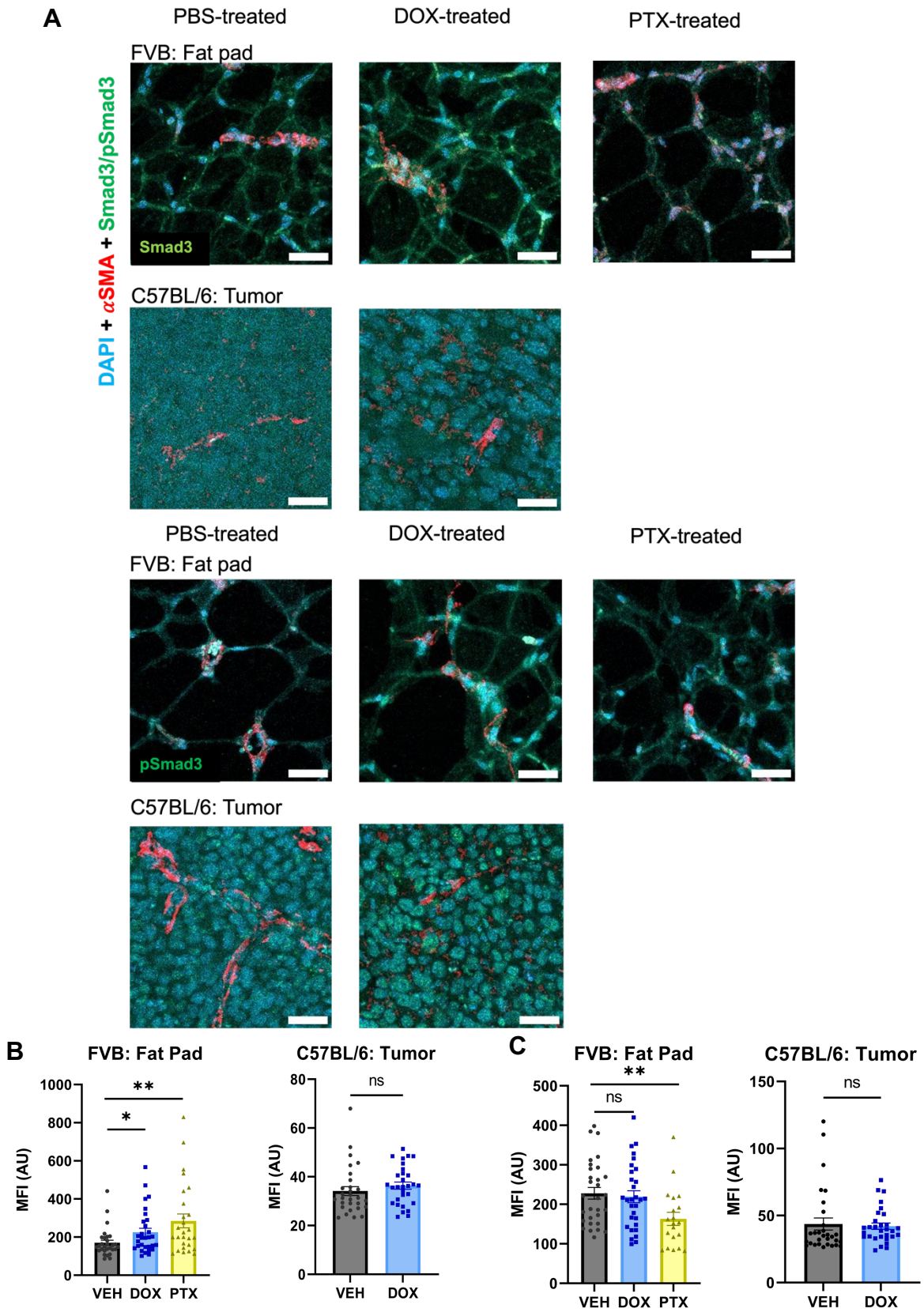

Figure 3.3 Effect of chemotherapy on phosphorylation of Smad3 in fibroblasts. (A) Representative images of FVB fat pads and C57 tumors stained for Smad3/pSmad3 (green), α-SMA (red) and DAPI (blue). Scale bar: 50μm. Quantification of Smad3 (B) and pSmad3 (C). Data are shown as mean with SEM, each data point represents the mean of one field of view per animal. n=3 animals per group.

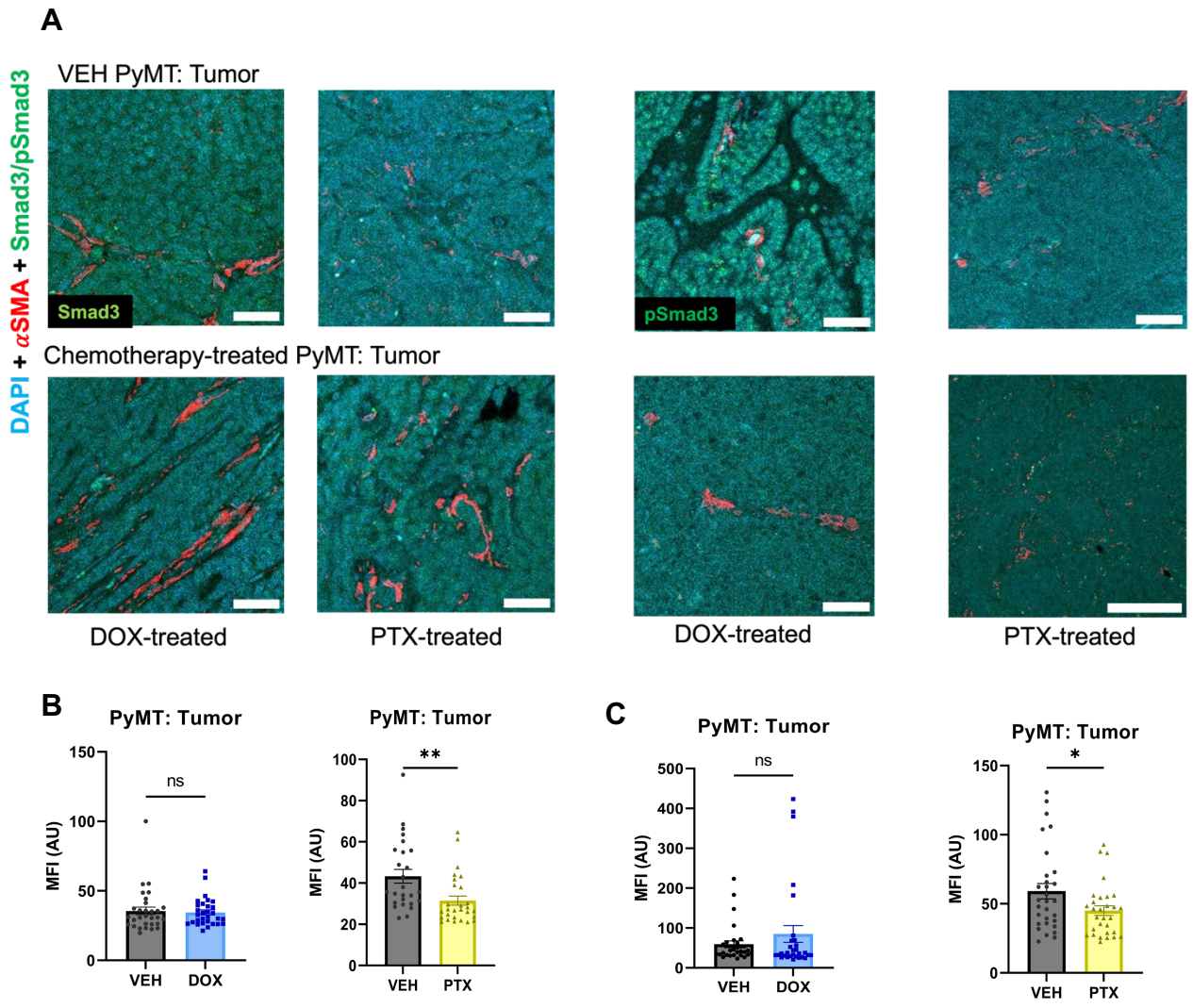

Figure 3.4 Effect of chemotherapy on phosphorylation of Smad3 in fibroblasts from MMTV-PyMT tumors. (A) Representative images of PyMT tumors stained for Smad3/pSmad3 (green), α-SMA (red) and DAPI (blue). Scale bar: 50μm. Quantification of Smad3 (B) and pSmad3 (C). Data are shown as mean with SEM, each data point represents the mean of one field of view per animal. n=3 animals per group.

3.4 Discussion

Here, we aimed to better understand the effect of chemotherapy *in vivo* on fibroblast activation. First, my data show that there is no difference in Collagen IV and VI abundance between chemotherapy treatment and controls. There is a high level of heterogeneity within fibroblasts *in vivo*, so it can be challenging to evaluate fibroblast activation *in vivo*. I found that doxorubicin did induce an increase fibroblast activation as quantified by a-SMA positive area in orthotopic tumors. However, there was not comparably increase in spontaneous tumor. The underlying mechanism can be complex. First, orthotopic tumor progresses more rapidly than spontaneous tumor[55], indicating a higher baseline of fibroblast activation, injection created a wound-healing-like response and chemotherapy possibly enhanced it, leading to a stronger myofibroblast activation. In spontaneous tumor, chemotherapy distribution might be heterogeneous due to natural tumor structure, activating less consistent fibroblast activation, shown in the locational difference. Therefore, it will be feasible to investigate fibroblast activation based on location in spontaneous tumor.

In addition, I investigate the activation of Smad3 in chemotherapy-treated healthy and tumor-bearing tissue. I found that doxorubicin had no effect on Smad3 expression and activation in both orthotopic and spontaneous tumor tissues. In healthy tissue, chemotherapy increased Smad3 expression, but doxorubicin did not change Smad3 activation. While paclitaxel significantly inhibited Smad3 phosphorylation in both healthy fat pads and spontaneous tumors. Smad3 is a key factor in TGF-β-mediated fibroblast activation, which promotes tumor progression and metastasis when increases[31,33]. I was unable to look at both Smad3 and phosphorylated Smad3 simultaneously in the same

tumor section, and calculating the phosphorylation ratio could provide a more accurate characterization of Smad3 activation. It is also possible that other mechanisms of activation are important here, considering that Smad3 signaling is only one pathway among many mechanisms known to drive fibroblast activation.

Further, I found some very interesting differences in fibroblast abundance depending on the location of the tumor, especially for the spontaneous tumors. Fibroblasts play an important role in enhancing chemoresistance by forming a physical barrier at the tumor periphery. Chemotherapy activates fibroblasts at peripherical tumor, the resulting tumor architecture, in turn, restricts drug penetration into the central tumor regions, thereby promoting drug resistance and supporting tumor progression. Understanding the mechanisms underlying activated fibroblast peripheralization may offer valuable insights into improving prognosis by inhibiting fibroblast activation.

Overall, these data measured the expression of α-SMA and Smad3/pSmad3 with observed trend indicates that chemotherapy potentially contributes to the alteration of ECM components and fibroblast activation. As a result, to further investigate how chemotherapy impacts fibroblast activation in both tumor and healthy fat pads, using more specific markers for fibroblast activation, looking at a range of pathways that drive activation, but also utilizing AC-T-treated mouse which more accurately replicate the human treatment regimen.

3.5 Contributions to this chapter

Conception and design: Madeleine J. Oudin, Anna Yui, Liyi Peng

Resources: Jackson P. Fatherree, Abraham Bayer, Justinne R. Guarin, Anna Yui, Hannah B. Borges

Acquisition of data: Liyi Peng

Analysis and interpretation of data (e.g., statistical analysis, biostatistics, computational analysis): Liyi Peng, Anna Yui, Thomas Gerton

Writing, review, and/or revision of the manuscript: Liyi Peng, Anna Yui, Madeleine J. Oudin

Chapter 4: Conclusions and Future Directions

TNBC accounts for about 10-15% of all breast cancer cases with an aggressive phenotype, and the 5-year survival rate of localized TNBC is approximately 77% and patients have high risk experiencing recurrence and metastasis. All TNBC patients will receive chemotherapy[13] and immunotherapy, which is only available for a subset of patients. It is essential to understand the mechanisms of chemoresistance in order to optimize current regimen and improve outcomes for patients.

Due to the physical and functional impacts on surrounding cells, the ECM has been recognized as a key factor in regulation of various diseases, especially cancer. In cancer, the ECM has been reported to not only support tumor formation by providing tumor cell adhesion sites, but also work as a highly dynamic network to promote tumor growth and progression through depositing, remodeling and signaling[24,38]. The compositions of ECM, have been demonstrated to change post chemotherapy, collectively driving breast cancer cell invasion[30,52]. Further preliminary data showed that fibroblast, the primary producer of ECM, is activated by chemotherapy drugs.

The goal of this dissertation was to further investigate how chemotherapy can affect fibroblast activation and the ECM they produce, leading to the influence on TNBC tumor invasion. To simulate the clinical regimen, I evaluated the fibroblast activation after treating fibroblast with a sequential *in vitro* treatment. These results showed that an increase of α-SMA and elongation in AC-T-treated fibroblast, indicating AC-T therapy significantly induce fibroblast activation. Each drug had different impact on Smad3 signaling pathway of fibroblasts, and there was no significant difference in fibroblasts treated with AC-T. Additionally, insight on long-term effect of chemotherapy drugs was

provided based on the difference between single-drug and sequential treatment. Since AC-T therapy consists of two distinct treatment phases (AC phase and Taxol phase), drugs can be administered at different time points to investigate the timing effects on Smad3 activation in fibroblasts. For example, DOX and PM can be added during the taxol phase and compared to administration during the AC phase. Additionally, using inhibitors targeting potential signaling pathways associated with fibroblast activation can help identify the primary drivers of fibroblast-induced pro-invasive changes in the ECM following chemotherapy. Exploring the effects of other pathways, such as Hedgehog signaling[34,53], could provide a more comprehensive understanding of fibroblast activation.

While previous *in vitro* studies demonstrated significant fibroblast activation upon chemotherapy treatment, in this work, doxorubicin significantly increased fibroblast activation in orthotopic tumor. However, chemotherapy treatment did not significantly alter α-SMA area or Smad3 phosphorylation in healthy fat pads or spontaneous tumor tissues, suggesting the underlying mechanisms of pro-invasive changes in TNBC tumor ECM needs further investigation for better understanding. Due to the more rapid tumor progression and active interaction within the tumor microenvironment[55], the formation of orthotopic tumor may enhance fibroblast activation, amplifying the effect of chemotherapy on fibroblasts. Both previous study and the *in vitro* experiments in this work showed that the signaling pathways activated by chemotherapy drugs are complex, but together they promote fibroblast activation. Therefore, it is critical to utilize AC-T-treated mouse models for optimal simulation. Combining fibroblast activation data from both orthotopic and spontaneous tumor models can provide a more comprehensive perspective about the effect of chemotherapy. To characterize fibroblast activation in vivo, AC-T-treated mouse

tissues can be used for immunostaining to analyze the expression of fibroblast activation biomarkers. It will be possible to calculate phosphorylation ratio within tissue by imaging entire tissue section. Using PyMT mouse model will allow to explore the locational difference of fibroblast activation. Also, focusing on fibroblasts at the periphery of spontaneous tumor will enable further evaluation about the effects of chemotherapy on fibroblast activation in a more reliable and precise way. The mouse tissues can also be decellularized and reseed them with TNBC cells to further assess how AC-T therapy affects cell motility. The combination of these experiments could provide insights into the mechanism of chemoresistance and invasion, aiming to optimize chemotherapy strategies.

Reference

1. Sung, H., Ferlay, J., Siegel, R. L., Laversanne, M., Soerjomataram, I., Jemal, A., & Bray, F. (2021). Global cancer statistics 2020: GLOBOCAN estimates of incidence and mortality worldwide for 36 cancers in 185 countries. CA: A Cancer Journal for Clinicians, 71(3), 209–249.
2. American Cancer Society. (2025, January 22). How common is breast cancer? American Cancer Society.
3. American Cancer Society. Breast Cancer Facts and Figures 2024-2025. Atlanta: American Cancer Society; 2024.
4. Orrantia-Borunda, E., Anchondo-Nuñez, P., Acuña-Aguilar, L. E., et al. (2022, August 6). Subtypes of breast cancer. In H. N. Mayrovitz (Ed.), Breast Cancer (Chapter 3). Exon Publications.
5. Siegel, R. L., Miller, K. D., Fuchs, H. E., & Jemal, A. (2024). Cancer statistics, 2024. CA: A Cancer Journal for Clinicians, 74(2), 106–133.
6. American Cancer Society. (2023, March 1). Triple-negative breast cancer. American Cancer Society.
7. Kesireddy, M., Elsayed, L., Shostrom, V. K., Agarwal, P., Asif, S., Yellala, A., & Krishnamurthy, J. (2024). Overall survival and prognostic factors in metastatic triple-negative breast cancer: A National Cancer Database analysis. Cancers, 16(10), 1791.
8. National Cancer Institute. (2024). Breast cancer treatment (PDQ®)–Patient version.
9. American Cancer Society. (2025, January 16). Breast cancer survival rates. American Cancer Society.
10. O'Reilly, D., Sendi, M. A., & Kelly, C. M. (2021). Overview of recent advances in metastatic triple negative breast cancer. World journal of clinical oncology, 12(3), 164–182.
11. Obidiro, O., Battogtokh, G., & Akala, E. O. (2023). Triple Negative Breast Cancer Treatment Options and Limitations: Future Outlook. Pharmaceutics, 15(7), 1796.
12. Yin, L., Duan, J. J., Bian, X. W., & Yu, S. C. (2020). Triple-negative breast cancer molecular subtyping and treatment progress. Breast cancer research : BCR, 22(1), 61.
13. National Comprehensive Cancer Network. (2025). NCCN Clinical Practice Guidelines in Oncology: Breast Cancer (Version 3.2025).
14. Vriens, B. E. P. J., Vriens, I. J. H., Aarts, M. J. B., van Gastel, S. M., van den Berkmortel, F. W. P. J., Smilde, T. J., van Warmerdam, L. J. C., van Spronsen, D. J., Peer, P. G. M., de Boer, M., Tjan-Heijnen, V. C. G., & Breast Cancer Trialists' Group of the Netherlands (BOOG) (2017). Improved survival for sequentially as opposed to concurrently delivered neoadjuvant chemotherapy in non-metastatic breast cancer. Breast cancer research and treatment, 165(3), 593–600.
15. Fujii, T., Le Du, F., Xiao, L., Kogawa, T., Barcenas, C. H., Lu, C., ... & Hortobagyi, G. N. (2015). Effectiveness of an Adjuvant Chemotherapy Regimen for Early-Stage Breast Cancer: A Systematic Review and Network Meta-analysis. JAMA Oncology, 1(9), 1311–1318.
16. National Comprehensive Cancer Network Clinical Practice Guidelines in Oncology. 2015.
17. De Laurentiis M, Cancello G, D'Agostino D, et al. Taxane-based combinations as adjuvant chemotherapy of early breast cancer: a meta-analysis of randomized trials. J Clin Oncol. 2008;26(1):44-53.
18. Gandhi S, Fletcher GG, Eisen A, et al. Adjuvant chemotherapy for early female breast cancer: a systematic review of the evidence for the 2014 Cancer Care Ontario systemic therapy guideline. Curr Oncol. 2015;22(suppl 1):S82-S94.
19. Mamounas, E. P., Bryant, J., Lembersky, B., Fehrenbacher, L., Sedlacek, S. M., Fisher, B., Wickerham, D. L., Yothers, G., Soran, A., & Wolmark, N. (2005). Paclitaxel after doxorubicin plus cyclophosphamide as adjuvant chemotherapy for node-positive breast cancer: Results from NSABP B-28. Journal of Clinical Oncology, 23(16), 3686–3696.

20. Vriens, B. E., Aarts, M. J., de Vries, B., van Gastel, S. M., Wals, J., Smilde, T. J., van Warmerdam, L. J., de Boer, M., van Spronsen, D. J., Borm, G. F., Tjan-Heijnen, V. C., & Breast Cancer Trialists' Group of the Netherlands (BOOG) (2013). Doxorubicin/cyclophosphamide with concurrent versus sequential docetaxel as neoadjuvant treatment in patients with breast cancer. European journal of cancer (Oxford, England : 1990), 49(15), 3102–3110.
21. Carey, L. A., Dees, E. C., Sawyer, L., Gatti, L., Moore, D. T., Collichio, F., Ollila, D. W., Sartor, C. I., Graham, M. L., & Perou, C. M. (2007). The triple negative paradox: primary tumor chemosensitivity of breast cancer subtypes. Clinical cancer research : an official journal of the American Association for Cancer Research, 13(8), 2329–2334.
22. Stewart, R. L., Updike, K. L., Factor, R. E., Henry, N. L., Boucher, K. M., Bernard, P. S., & Varley, K. E. (2019). A Multigene Assay Determines Risk of Recurrence in Patients with Triple-Negative Breast Cancer. Cancer research, 79(13), 3466–3478.
23. Nedeljković, M., & Damjanović, A. (2019). Mechanisms of Chemotherapy Resistance in Triple-Negative Breast Cancer-How We Can Rise to the Challenge. Cells, 8(9), 957.
24. Anderson, N. M., & Simon, M. C. (2020). The tumor microenvironment. Current biology: CB, 30(16), R921–R925.
25. Deepak, K. G. K., Vempati, R., Nagaraju, G. P., Dasari, V. R., S, N., Rao, D. N., & Malla, R. R. (2020). Tumor microenvironment: Challenges and opportunities in targeting metastasis of triple negative breast cancer. Pharmacological research, 153, 104683.
26. Bussard, K. M., Mutkus, L., Stumpf, K., Gomez-Manzano, C., & Marini, F. C. (2016). Tumor-associated stromal cells as key contributors to the tumor microenvironment. Breast cancer research : BCR, 18(1), 84.
27. Öhlund, D., Handly-Santana, A., Biffi, G., Elyada, E., Almeida, A. S., Ponz-Sarvise, M., Corbo, V., Oni, T. E., Hearn, S. A., Lee, E. J., Chio, I. I., Hwang, C. I., Tiriac, H., Baker, L. A., Engle, D. D., Feig, C., Kultti, A., Egeblad, M., Fearon, D. T., Crawford, J. M., … Tuveson, D. A. (2017). Distinct populations of inflammatory fibroblasts and myofibroblasts in pancreatic cancer. The Journal of experimental medicine, 214(3), 579–596.
28. Martin, O. A., Anderson, R. L., Narayan, K., & MacManus, M. P. (2017). Does the mobilization of circulating tumour cells during cancer therapy cause metastasis?. Nature reviews. Clinical oncology, 14(1), 32–44.
29. Karagiannis, G. S., Condeelis, J. S., & Oktay, M. H. (2019). Chemotherapy-Induced Metastasis: Molecular Mechanisms, Clinical Manifestations, Therapeutic Interventions. Cancer research, 79(18), 4567–4576.
30. Fatherree, J. P., Guarin, J. R., McGinn, R. A., Naber, S. P., & Oudin, M. J. (2022). Chemotherapy- Induced Collagen IV Drives Cancer Cell Motility through Activation of Src and Focal Adhesion Kinase. Cancer research, 82(10), 2031–2044.
31. Millet, C., & Zhang, Y. E. (2007). Roles of Smad3 in TGF-beta signaling during carcinogenesis. Critical reviews in eukaryotic gene expression, 17(4), 281–293.
32. Kojima, Y., Acar, A., Eaton, E. N., Mellody, K. T., Scheel, C., Ben-Porath, I., Onder, T. T., Wang, Z. C., Richardson, A. L., Weinberg, R. A., & Orimo, A. (2010). Autocrine TGF-β and stromal cell-derived factor-1 (SDF-1) signaling drives the evolution of tumor-promoting mammary stromal myofibroblasts. Proceedings of the National Academy of Sciences of the United States of America, 107(46), 20009–20014.
33. Dobaczewski, M., Bujak, M., Li, N., Gonzalez-Quesada, C., Mendoza, L. H., Wang, X. F., & Frangogiannis, N. G. (2010). Smad3 signaling critically regulates fibroblast phenotype and function in healing myocardial infarction. Circulation research, 107(3), 418–428.
34. Peiris-Pagès, M., Sotgia, F., & Lisanti, M. P. (2015). Chemotherapy induces the cancer-associated fibroblast phenotype, activating paracrine Hedgehog-GLI signalling in breast cancer cells. Oncotarget, 6(13), 10728–10745.

35. Heenatigala Palliyage, G., Samart, P., Bobbala, S., Rojanasakul, L. W., Coyle, J., Martin, K., Callery, P. S., & Rojanasakul, Y. (2023). Chemotherapy-induced PDL-1 expression in cancer-associated fibroblasts promotes chemoresistance in NSCLC. Lung Cancer, 181, 11–20.
36. Glabman, R. A., Choyke, P. L., & Sato, N. (2022). Cancer-Associated Fibroblasts: Tumorigenicity and Targeting for Cancer Therapy. Cancers, 14(16), 3906.
37. Franco-Barraza, J., Raghavan, K. S., Luong, T., & Cukierman, E. (2020). Engineering clinically-relevant human fibroblastic cell-derived extracellular matrices. Methods in cell biology, 156, 109–160.
38. Huang, J., Zhang, L., Wan, D. et al. Extracellular matrix and its therapeutic potential for cancer treatment. Sig Transduct Target Ther 6, 153 (2021).
39. Zhang, H., Yue, X., Chen, Z. et al. Define cancer-associated fibroblasts (CAFs) in the tumor microenvironment: new opportunities in cancer immunotherapy and advances in clinical trials. Mol Cancer 22, 159 (2023).
40. Cleveland Clinic. (2022). Immunotherapy side effects. Cleveland Clinic.
41. Sriramulu, S., Thoidingjam, S., Speers, C., & Nyati, S. (2024). Present and Future of Immunotherapy for Triple-Negative Breast Cancer. Cancers, 16(19), 3250.
42. Li, L., Zhang, F., Liu, Z., & Fan, Z. (2023). Immunotherapy for Triple-Negative Breast Cancer: Combination Strategies to Improve Outcome. Cancers, 15(1), 321.
43. Hargadon, K. M., Johnson, C. E., & Williams, C. J. (2018). Immune checkpoint blockade therapy for cancer: An overview of FDA-approved immune checkpoint inhibitors. International immunopharmacology, 62, 29–39.
44. Kuperwasser, C., Chavarria, T., Wu, M., Magrane, G., Gray, J. W., Carey, L., Richardson, A., & Weinberg, R. A. (2004). Reconstruction of functionally normal and malignant human breast tissues in mice. Proceedings of the National Academy of Sciences of the United States of America, 101(14), 4966–4971.
45. Gomes, R.N., Manuel, F. & Nascimento, D.S. The bright side of fibroblasts: molecular signature and regenerative cues in major organs. npj Regen Med 6, 43 (2021).
46. Akhmetshina, A., Palumbo, K., Dees, C. et al. Activation of canonical Wnt signalling is required for TGF-β-mediated fibrosis. Nat Commun 3, 735 (2012).
47. Fuertes, G., Del Valle-Pérez, B., Pastor, J., Andrades, E., Peña, R., García de Herreros, A., & Duñach, M. (2023). Noncanonical Wnt signaling promotes colon tumor growth, chemoresistance and tumor fibroblast activation. EMBO reports, 24(4), e54895.
48. Wu, F., Yang, J., Liu, J. et al. Signaling pathways in cancer-associated fibroblasts and targeted therapy for cancer. Sig Transduct Target Ther 6, 218 (2021).
49. Mori, Y., Okimoto, Y., Sakai, H., Kanda, Y., Ohata, H., Shiokawa, D., Suzuki, M., Yoshida, H., Ueda, H., Sekizuka, T., Tamura, R., Yamawaki, K., Ishiguro, T., Mateos, R. N., Shiraishi, Y., Yatabe, Y., Hamada, A., Yoshihara, K., Enomoto, T., & Okamoto, K. (2024). Targeting PDGF signaling of cancer-associated fibroblasts blocks feedback activation of HIF-1α and tumor progression of clear cell ovarian cancer. Cell reports. Medicine, 5(5), 101532.
50. Cescon M, Gattazzo F, Chen P, Bonaldo P (2015) Collagen VI at a glance. J Cell Sci 128:3525–3531.
51. Kuo H-J, Maslen CL, Keene DR, Glanville RW (1997) Type VI collagen anchors endothelial basement membranes by interacting with type IV collagen. J Biol Chem 272:26522–26529.
52. Wishart, A. L., Conner, S. J., Guarin, J. R., Fatherree, J. P., Peng, Y., McGinn, R. A., Crews, R., Naber, S. P., Hunter, M., Greenberg, A. S., & Oudin, M. J. (2020). Decellularized extracellular matrix scaffolds identify full-length collagen VI as a driver of breast cancer cell invasion in obesity and metastasis. Science advances, 6(43), eabc3175.
53. Habib, J. G., & O'Shaughnessy, J. A. (2016). The hedgehog pathway in triple-negative breast cancer. Cancer medicine, 5(10), 2989–3006.

54. Caligiuri, G., & Tuveson, D. A. (2023). Activated fibroblasts in cancer: Perspectives and challenges. Cancer cell, 41(3), 434–449.
55. Onaciu, A., Munteanu, R., Munteanu, V. C., Gulei, D., Raduly, L., Feder, R. I., Pirlog, R., Atanasov, A. G., Korban, S. S., Irimie, A., & Berindan-Neagoe, I. (2020). Spontaneous and Induced Animal Models for Cancer Research. Diagnostics (Basel, Switzerland), 10(9), 660.